

1 **Were Phanerozoic (micro)continent-continent collisions frontal or**  
2 **oblique? Possible criteria and the Devonian collision of Chilenia**  
3 **with SW Gondwana as an example**  
4  
5

6 Hans-Joachim Massonne<sup>1,2</sup>, Botao Li<sup>1</sup>

7  
8 <sup>1</sup> State Key Laboratory of Geological Processes and Mineral Resources, School of Earth and  
9 Planetary Sciences, China University of Geosciences, 388 Lumo Road, 430074 Wuhan, China

10 <sup>2</sup> Fakultät Chemie, Universität Stuttgart, Pfaffenwaldring 55, 70569 Stuttgart, Germany  
11  
12

13 **Corresponding author:**

14 Hans-Joachim Massonne, e-mail: [h-j.massonne@mineralogie.uni-stuttgart.de](mailto:h-j.massonne@mineralogie.uni-stuttgart.de), ORCID: 0000-  
15 0002-2826-4767

16 Second author: Botao Li, e-mail: [libotao123@hotmail.com](mailto:libotao123@hotmail.com), ORCID: 0000-0003-4851-8928  
17  
18  
19

20 **Abstract**

21 The understanding of ancient continent-continent collisions requires information on the type of  
22 accretion (frontal or oblique) of the colliding plates. The shape of the P-T path of a rock, which  
23 was metamorphosed during ongoing continent-continent collision, has so far been ignored to  
24 obtain this information. However, the consideration of corresponding P-T paths related to  
25 Phanerozoic orogens suggests that the shape of the burial path has the potential to distinguish  
26 between frontal (60–90° angle between collisional front and plate convergence direction) and  
27 oblique (<45°) collisions. In case of an oblique collision, the P-T path is nearly isothermal towards  
28 peak-pressure conditions. These conditions should be in the range of 12–20 kbar although  
29 somewhat higher pressures cannot be excluded. In this contribution, this finding is applied  
30 exemplary to the collision of SW Gondwana with microcontinent Chilenia being part of the  
31 Palaeozoic collage of microcontinents in the southern part of South America. However, only a  
32 single P-T path of a metasediment (Guarguaraz Complex) in the literature provides the requested  
33 information. This path is characterized by nearly isothermal burial reaching peak pressures of ~14  
34 kbar at about 480 °C. Thus, it is suggested that the approach of Chilenia to Gondwana was oblique.  
35 The abundance of serpentinite bodies in the Guarguaraz Complex is not in conflict with this  
36 suggestion.

37 **Keywords:** Continent-continent collision, Chilenia, Gondwana, P-T evolution, garnet,

38

39

40

41

42 **¿Fueron frontales u oblicuas las colisiones (micro)continente-continente del Fanerozoico?**  
43 **Posibles criterios y la colisión devónica de Chilenia con el suroeste de Gondwana como**  
44 **ejemplo.**

45 La comprensión de antiguas colisiones continente-continente requiere información sobre el tipo  
46 de acreción (frontal u oblicua) de las placas en colisión. La forma de la trayectoria P-T de rocas  
47 metamorizadas durante la colisión no ha sido considerada previamente para este propósito. Sin  
48 embargo, el análisis de trayectorias P-T en orógenos fanerozoicos sugiere que la forma de la  
49 trayectoria de enterramiento permite distinguir entre colisiones frontales (ángulo de 60–90° entre  
50 el frente de colisión y la dirección de convergencia de las placas) y oblicuas (<45°). En colisiones  
51 oblicuas, esta etapa de la trayectoria P-T es casi isotérmica hacia condiciones de presión máxima,  
52 típicamente en el rango de 12–20 kbar, aunque no se descartan valores mayores. En esta  
53 contribución, este enfoque se aplica a la colisión del suroeste de Gondwana con el microcontinente  
54 Chilenia, parte del ensamblaje paleozoico de microcontinentes en el sur de Sudamérica. No  
55 obstante, solo una trayectoria P-T publicada para un metasedimento del Complejo Guarguaraz  
56 proporciona la información requerida. Esta trayectoria muestra un enterramiento casi isotérmico,  
57 que alcanzó presiones máximas de ~14 kbar a ~480 °C. Estos resultados sugieren que la  
58 aproximación de Chilenia a Gondwana fue oblicua. La abundancia de cuerpos de serpentinitas en  
59 el Complejo Guarguaraz no contradice esta interpretación.

60 **Palabras clave.** Colisión continente-continente; Chilenia; Gondwana; evolución P-T; granate

61

62

## 63 Introduction

64 Continent-continent collisions have taken place on Earth for a long time and led to numerous  
65 orogenic belts. As these collisions and belts are the results of drifting continental plates, the  
66 reconstructions of these past drifts require reliable criteria, of which data of palaeomagnetic  
67 measurements are important ones (e.g., van der Voo, 1990; Dallanave, 2024). Other criteria such  
68 as the timing of opening and closure of subducted oceanic plates also provide constraints for these  
69 reconstructions (e.g., Stampfli, 2000; Müller et al., 2018). However, the available data are hardly  
70 precisely enough to reach palaeogeographic reconstructions, which are sufficiently reliable even  
71 for the younger Earth's history of the late Phanerozoic.

72 The type of continent-continent collision with respect to the convergence of continental plates  
73 leading either to frontal (60–90° angle between collisional front and the direction of the  
74 convergence of plates) or oblique (<45°) collisions is one of the problems in the plate  
75 reconstructions for the Phanerozoic. Usually, these collisions are considered to be frontal ones, but  
76 it will be shown later (see Section 2.1) that significantly oblique collisions are also common.  
77 Obliquely convergent plate boundaries are typically characterized by orogenic zones, which are  
78 bounded by major strike-slip faults oriented (sub)parallel to the plate boundary (Teyssier et al.,  
79 1995). In this study, it is worked out what type of P-T trajectory is typical for rocks, which were  
80 part of a downgoing crust resulting from oblique continent-continent collision. It will be  
81 demonstrated that a nearly isothermal burial path is typical for this kind of collision.

82 The above finding is applied to SW South America. The question that remained unanswered  
83 for this region is how (i.e., frontal or oblique) the various microplates, of which this area is mainly  
84 composed (e.g., Ramos, 1988; Dalziel, 1997; Heredia and Folguera, 2025; see also Section 3.1),  
85 collided with Gondwana in the Palaeozoic. We refer here to the example of the Devonian collision

86 of microcontinent Chilenia with SW Gondwana trying to answer the question whether this  
87 collision was frontal or oblique. Based on the criterion of a nearly isothermal burial path of a  
88 metasediment from the Guarguaraz Complex (Massonne and Calderón, 2008), an oblique  
89 Chilenia-Gondwana collision is suggested here.

## 90 **Scenarios of Phanerozoic plate collisions including typical P-T paths**

### 91 General situation

92 The Cenozoic collision of the Indian and Eurasian plates is considered to be the most typical  
93 continent-continent one that has led to an impressive orogen: the Himalayan ranges (Fig. 1). This  
94 orogen resulted from a frontal collision after the Tethys ocean floor between these continental  
95 plates was completely subducted. High-pressure (HP: >10 kbar) rocks formed still during this  
96 subduction. These rocks are important for the reconstruction of the collisional evolution, which is  
97 shown in the sketch of figure 2A. Rocks from the deeply subducted oceanic crust, eclogites and  
98 related rock types, were partly exhumed in the deep subduction channel and belong to the oldest  
99 rocks of the Cenozoic metamorphism (ca. 50 Ma) in the Himalayas (e.g., Massonne and O'Brien,  
100 2003). The corresponding P-T path is shown in figure 2B (yellow line). This path reached  
101 ultrahigh-pressure (UHP) conditions (e.g.,  $\geq 28$  kbar at 700 °C) as documented by relics of the SiO<sub>2</sub>  
102 polymorph coesite found in Himalayan eclogite (O'Brien et al., 2001). Another P-T path exhibited  
103 in figure 2B (dark orange line) is related to an accretionary wedge system assumed to have formed  
104 at the margin of the Eurasian plate, which later collided with India. This path was taken from  
105 studies of the Palaeozoic accretionary complexes in Chile (and is addressed in Section 3.2). A third  
106 P-T path in figure 2B (cyan line) is related to a representative rock in the upper portion of the  
107 downgoing Indian plate that is presently (significantly later than stage III in figure 2A) at the

108 Earth's surface due to tectonic processes. Derived peak pressures for such rocks are between 10  
109 and 14 kbar (see Liu et al., 2007; Iaccarino et al., 2015) at temperatures above 600 °C. Other  
110 authors (e.g., Kaneko et al., 2003; Palin et al., 2017), however, assumed a deep burial of the Indian  
111 crust to depth of up to 100 km (equivalent to ~30 kbar lithostatic pressure).

112 A careful look at figure 1 reveals that, besides the Himalayan ranges, additional orogens  
113 formed by the India-Eurasia collision that are characterized by the appearance of ophiolite belts  
114 with significant proportions of serpentinite bodies (e.g., Ovington et al., 2021). Focusing on the  
115 orogen, in which the Burma microplate was involved, the corresponding ranges are most likely  
116 related to an oblique continent-continent collision also discernible by a major transpressional  
117 strike-slip fault system (Rangin et al., 2013; Naing et al., 2023). Among the rocks in Myanmar that  
118 are exposed near such a major fault are, for example, HP rocks of the blueschist facies (P-T  
119 conditions of 16–19 kbar and 470–540 °C; Nyunt et al., 2017; pressure conditions of 12–17 kbar  
120 for jadeitite; Harlow et al., 2015).

#### 121 Cenozoic plate collision forming the European Alps

122 The European Alps might be the best studied orogen on Earth. However, this orogen is  
123 complicated (Dal Piaz et al., 2003; Handy et al., 2010), because metamorphic rocks, which are  
124 characterized by P-T paths pointing to a frontal collision of microcontinent Adria (upper plate)  
125 with the European plate in the late Eocene (e.g., Bonnet et al., 2022), occur only in the Western  
126 Alps. In this part of the Alps, rocks with P-T paths similar to the yellow one in figure 2B occur  
127 (e.g., Groppo et al., 2019). The same is true for rocks from the upper part of the subducted  
128 European plate with P-T conditions similar to the cyan path in figure 2B as derived, for example,  
129 by Massonne (2015), and those of the former accretionary wedge (Tricart and Schwartz, 2006;  
130 compare with the dark orange path in figure 2B). The Cenozoic evolution of the Eastern Alps

131 including (portions of) the Central Alps is different. The most plausible reason is that NE Adria  
132 collided with Europe obliquely (see Dewey et al., 1998). This type of collision leading to  
133 continental subduction was considered by Li et al. (2023) for the Eocene evolution of the Eastern  
134 Alps being compatible with: (1) a narrow ocean between eastern Adria and Europe at the beginning  
135 of the Cenozoic (see Agard and Handy, 2021); (2) the occurrence of a major strike-slip fault  
136 system, the Periadriatic Fault System (Handy et al., 2005); and (3) the appearance of ultrabasic  
137 bodies close to this fault system (e.g., De Hoog et al., 2009). The corresponding P-T path for the  
138 Eocene evolution of a metasediment from the Eastern Alps (Pohorje Mountains; Li et al., 2021),  
139 assigned to the European plate, is shown in figure 3 (black path). This path is characterized by  
140 nearly isothermal burial to peak-pressure conditions of 20 kbar at about 580 °C.

#### 141 Palaeozoic oblique plate collisions in Europe and NE North America

142 Oblique continent-continent collisions have also been proposed for Palaeozoic orogens in  
143 Europe (Kroner et al., 2016; for the Variscan orogen in general: e.g., Franke, 2000) and NE North  
144 America (Appalachian orogen in Canada in general: Williams, 1979; van Staal et al., 2009). Both  
145 orogens are characterized by the occurrence of major transpressive strike-slip fault systems.

146 A studied rock in Newfoundland (eclogite; Massonne, 2024a), part of the downgoing margin  
147 of Laurentia, crops out close to the Baie Verte Line (Slavinski et al., 2010), which is a major shear  
148 zone. Larger serpentinite bodies occur at this shear zone as well. The addressed eclogite was  
149 metamorphosed during the Taconic orogeny in the Early to Middle Ordovician (van Staal and  
150 Zagorevski, 2020). The burial P-T path of this rock is characterized again by nearly isothermal  
151 burial. Peak-pressure conditions were approximately 19 kbar at 570 °C (light grey path in figure  
152 3).

153 Metamorphic rocks, for which burial paths could be reconstructed, are also very rare in the

154 well-studied Variscan orogen. Two examples are presented. An eclogite from the southern  
155 Armorican massif in France was studied by Massonne and Li (2022). This rock occurs in the Les  
156 Essarts HP unit of the Vendean zone (Godard, 2001), close to a major fault system. In this unit,  
157 ultrabasic and eclogitic rocks form km-sized bodies boudinaged parallel to this system. These  
158 rocks experienced HP metamorphism in the Devonian together with the surrounding gneisses  
159 (Bosse et al., 2024). The HP metamorphism at peak pressures of 20 kbar was reached at 570 °C  
160 by nearly isothermal burial (Massonne and Li, 2022). Another rock, a metasediment that  
161 experienced a similar P-T path (grey path in figure 3) with peak-pressure conditions of 17 kbar  
162 (Massonne, 2024b), occurs in the Erzgebirge Crystalline Complex (Germany-Czech Republic).  
163 The location of this rock in the Gneiss-Eclogite Unit of this complex is, in fact, not very close to  
164 ultrabasic bodies and a major strike-slip fault system of the Variscan orogen, but a nearly  
165 isothermal burial path was suggested to reach the peak-pressure conditions at 338 Ma. This age is  
166 common in the Erzgebirge Crystalline Complex (see Kröner and Willner, 1998; Werner and  
167 Lippolt, 2000). The aforementioned peak P-T conditions can also be related to gneiss (Kryl et al.,  
168 2021), the typical rock type in the Gneiss-Eclogite Unit, and eclogite bodies therein (Massonne,  
169 2011).

## 171 **Concise overview of the geological setting of Chile-Argentina in the Palaeozoic**

### 172 Plate collage

173 The southern part of South America is a collage of microplates (see figure 4) that were  
174 accreted to Gondwana predominantly in Palaeozoic times (Rapalini, 2005). The relative positions  
175 of these microplates are broadly accepted (cf. Ramos, 1988; Hervé et al., 2018). The same concerns  
176 the timing of the accretion of microplates to the west of the Rio de la Plata Craton. Pampia and

177 Cuyania reached their present positions in Cambrian to Silurian times (e.g., Vujovich et al., 2004;  
178 Casquet et al., 2018, 2021). Chilenia followed in the Devonian (Mpodozis and Ramos, 1990;  
179 Willner et al., 2011). Nevertheless, the Palaeozoic orogenic evolution of the margin of SW  
180 Gondwana is one of the most debated subjects in the southern part of South America, since  
181 contrasting palaeotectonic scenarios of (micro)continent-continent collisions have been proposed  
182 in the last decades (Marcos et al., 2023, and references therein). For example, the boundaries  
183 between these microplates are still under debate (Heredia and Folguera, 2025), mainly because the  
184 addressed region is partly covered by Cenozoic and late Mesozoic sedimentary and igneous rocks.  
185 More difficult to assess is the original position of these microplates that travelled and were  
186 subsequently attached to SW Gondwana. For instance, it was speculated that Cuyania was  
187 originally part of Laurentia and separated from Gondwana by a wide ocean (Thomas and Astini,  
188 1996: accretion at ~455 Ma). Another but similar plate constellation with a narrow ocean was  
189 envisaged by other researchers (e.g., Dalla Salda et al., 1992).

190 Another example relates to the accretion of Patagonia and the North Patagonian Massif (for  
191 locations see figure 4). This combined microplate collided with an already existing plate collage  
192 in Carboniferous to Early Permian times after rifting off another part of Gondwana (Rapalini et  
193 al., 2010). However, this part was assigned to different regions of Antarctica by Pankhurst et al.  
194 (2006) and Ramos and Naipauer (2014). In addition, Pankhurst et al. (2006) suggested that  
195 Patagonia and a microplate exposed in the North Patagonian Massif drifted separately and, thus,  
196 collided at different times with the supercontinent. Again, other views of the collisional situation  
197 appeared in the literature (e.g., Gregori et al., 2008, 2013).

198 Moreover, the assessment of the microplate configurations in southern South America at  
199 various times is impeded by additional factors. A major one is related to multiple collisional events,

200 which can have affected the accreted microplates and their suture zones (e.g., Serra-Varela et al.,  
201 2022; Bianchi et al., 2024).

## 202 Chilenia

203 Chilenia is part of the collage of microplates mentioned above (Fig. 4). Although some  
204 authors consider this microplate as hypothetical (e.g., Dahlquist et al., 2025), there are many  
205 arguments in the literature that suggest the existence of Chilenia (e.g., Willner et al., 2025).  
206 However, this microplate is almost not exposed, so its limits are broadly uncertain (see below). As  
207 this microplate is subject of our considerations, studies related to it are reviewed here in more  
208 detail.

209 Outcrops of the boundary region between Chilenia and Cuyania occur between latitudes 29–  
210 34° S. Metasediments and metabasites, which experienced relatively high peak pressures, and  
211 ultrabasic rocks such as serpentinites are typical for this boundary region (Boedo et al., 2021).  
212 Peak pressures of 7.0–9.3 kbar at temperatures around 370 °C were reported for metasediments  
213 and metabasites exposed between 32.1° and 32.2° S (Peñasco Formation; Boedo et al., 2016). The  
214 Guarguaraz Complex (Gregori and Bjerg, 1997; López and Gregori, 2004) in the Argentine Frontal  
215 Cordillera at around 33.4° S (same latitude as that of Santiago de Chile) is another outcropping  
216 boundary region. This complex is composed of metasediments, metamorphosed sills of basic  
217 rocks, and serpentinite bodies. The occurrence of basic and ultrabasic rocks and their geochemical  
218 signatures let López de Azarevich et al. (2009) to interpret them as part of Ordovician ophiolites  
219 (see also Davis et al., 1999). The medium-grade metasediments have a HP signature with peak-  
220 pressure conditions around 14 kbar at temperatures between 500 and 550 °C (red and green paths  
221 in figure 3; Massonne and Calderón, 2008; Willner et al., 2011) resulting from the Chilenia-  
222 Gondwana collisional event. This event in the Guarguaraz Complex was dated by Lu-Hf mineral

223 isochrons (garnet-hornblende in two amphibolites or garnet-white mica in a metapelite, two grain  
224 size fractions of one mineral and the whole rock) at  $390\pm 2$  Ma; a  $^{40}\text{Ar}/^{39}\text{Ar}$  plateau age (step heating  
225 of single, large phengite grains) of  $353\pm 1$  Ma was additionally obtained (Willner et al., 2011).

226 Similar Early-Mid Devonian zircon ages were also determined for rocks at latitude  $40^\circ$  S  
227 (north of San Carlos de Bariloche) by Varela et al. (2005). HP medium-grade metasediments that  
228 experienced peak-pressure conditions of 18 kbar were reported to occur at latitude  $41.2^\circ$  S  
229 (Colohuincul Complex), some km southwest of San Carlos de Bariloche (light blue path in figure  
230 3; Martínez et al., 2012). Th-U-Pb dating of monazite in these metasediments yielded ages of  
231  $391.7\pm 4.0$  and  $350.4\pm 5.8$  Ma (Martínez et al., 2012). Because of the coincidence of HP medium-  
232 grade metamorphism and late Palaeozoic ages of the metasediments at the Guarguaraz and  
233 Colohuincul complexes, the Chilenia-Gondwana collision was also assigned to metamorphic rocks  
234 close to San Carlos de Bariloche (Martínez et al., 2012). However, Oriolo et al. (2019) proposed  
235 peak metamorphic conditions of about  $650^\circ\text{C}$  and 11 kbar at  $\sim 300$  Ma (in situ Th-U-Pb monazite  
236 dating) for an area west of San Carlos de Bariloche.

237 Several Devonian calcalkaline plutons occur to the south of  $33^\circ$  S in the Frontal Cordillera,  
238 which were considered as part of a magmatic arc (Dahlquist et al., 2022). Devonian ages (U-Pb  
239 zircon,  $384\pm 3$  and  $383\pm 2$  Ma) were also reported from igneous rocks north of Chaitén (at latitudes  
240  $42.0^\circ$  and  $42.75^\circ$  S) by Hervé et al. (2016). These authors interpreted their results as evidence for  
241 the existence of a Devonian island arc chain that was located close to Patagonia and attached to  
242 this microcontinent later (Hervé et al., 2018). This island arc was called Chaitenia (Fig. 4). In fact,  
243 a relation to Chilenia was not regarded by Hervé et al. (2016, 2018), but it will be discussed in this  
244 study. At least, Plissart et al. (2026) considered Chaitenia as a back-arc system, the opening of  
245 which was linked to the Chilenia collision. Rocks formed by a Devonian magmatism were also

246 proved to occur at the south-western margin of the North Patagonian Massif (Rapela et al., 2021).  
247 West of Chilenia, no further continental plate was accreted, but the subduction of oceanic  
248 crust at least since the Carboniferous (e.g., Willner et al., 2005; Muñoz-Montecinos et al., 2024)  
249 has led to accretionary wedges (Hervé, 1988). The ages of the exposed accretionary complexes  
250 (see figure 4) are still late Palaeozoic at latitudes 38–43° S (e.g., Willner et al., 2005, Hervé et al.,  
251 2013). The dominant rock types in these fossil accretionary wedges are metamorphosed immature  
252 clastic sedimentary rocks, but basic rocks and relatively large km-sized slices of ultrabasic rocks  
253 (serpentinites) also occur (e.g., Plissart et al., 2019). Studies of these wedges in Chile have  
254 contributed to the understanding of their formation in general (e.g., Richter et al., 2007; Massonne  
255 and Willner, 2008). During a late evolution of an already thick accretionary wedge, basal accretion  
256 of various materials occurs, which are mainly foredeep sediments. Such rocks travel on top of the  
257 downgoing oceanic plate, being involved in the shallow subduction channel, and likely experience  
258 P-T conditions along a geotherm towards the peak conditions. These peak conditions are those of  
259 the blueschist facies (e.g., Willner et al., 2000; see also figure 2). It seems to be typical that the  
260 subducted rocks, which experienced the highest peak pressures (11–16 kbar), underwent a counter-  
261 clockwise P-T path in the Carboniferous accretionary complexes of Chile (Willner et al., 2004;  
262 Hyppolito et al., 2014; Plissart et al., 2026). A Carboniferous magmatic arc related to the  
263 subduction below Chilenia occurs in the Chilean Coastal Cordillera (Deckart et al., 2014; Maksaev  
264 et al., 2014); however, this arc might be displaced to the east by more than 100 km to occur south  
265 of 38° S on the Argentine side of the Andes (Yoya et al., 2023).

266

267

## 268 **Discussion**

### 269 General remarks

270 The frontal collision of India and Eurasia has formed a major orogen on Earth, but this  
271 collision was also accompanied by oblique continent-continent collisions (Section 2.1). Also, the  
272 Cenozoic formation of the European Alps was caused by the frontal (Western Alps) and oblique  
273 (Eastern Alps) collision of Adria with the European plate (Section 2.2). Thus, oblique continent-  
274 continent collisions must be common.

275 In Section 2, it was pointed out that such oblique collisions result in specific characteristics;  
276 among them is the part of the P-T path of a metamorphic rock that indicates nearly isothermal  
277 burial. A geodynamic model is presented in figure 5 that should explain what could cause this  
278 characteristic. The oblique approach of continental plates that are separated by a narrow oceanic  
279 basin (<500 km width), in fact, results in subduction of the (proto)oceanic crust but not in the  
280 evolution of a deep subduction channel, in which deeply subducted eclogite and related rocks are  
281 exhumed (Fig. 2A, yellow marker). It is assumed here that the subduction of an oceanic basin with  
282 a minimum width of 1,000 km can generate a corresponding channel flow. Consequently, UHP  
283 eclogites occur only in specific Phanerozoic orogens (here: Himalayan ranges, Western Alps; for  
284 other ones see, e.g., Gilotti, 2013), the formation of which was preceded by the subduction of an  
285 oceanic basin with sufficient width (>1,000 km). Orogens formed by oblique collision commonly  
286 lack UHP rocks. An exception is the above addressed Erzgebirge Crystalline Complex (Section  
287 2.3), where UHP rocks such as eclogite (Massonne, 2013) occur in the Gneiss-Eclogite Unit.  
288 However, these rocks were generated by UHP-HP crystallization of melts, which formed in the  
289 mantle after delamination of crustal material (see Massonne, 2023, and references therein).

290 After subduction of the (proto)oceanic crust during early oblique collision, continental crust

291 follows by a continental subduction process (Fig. 5, stage II) resulting in a steeply dipping  
292 subduction zone. For Cenozoic orogens, such a zone might still be discernible by a nearly vertically  
293 dipping high-velocity anomaly in the mantle as it was found beneath the Eastern Alps (Paffrath et  
294 al., 2021). Because of buoyancy forces, the continental crust (except some delaminated portions)  
295 should reach a maximum depth of 70 km (20 kbar lithostatic pressure), which was estimated  
296 according to the above considerations (see the P-T paths in figure 3).

297 It is important to discuss this maximum depth, because another process also leads to a P-T  
298 path characterized by nearly isothermal burial to great depths (>70 km) in Phanerozoic subduction  
299 zones. This process, called tectonic erosion, brings material from the upper continental plate into  
300 the subduction zone (Massonne and Li, 2020) as long as the collision of continental and oceanic  
301 plates is ongoing. For example, eclogite bodies occur in gneiss of the Malpica-Tuy zone as a result  
302 of the Variscan continent-continent collision in northwestern Spain. Such a body experienced a  
303 nearly isothermal burial path with peak-pressure conditions of 24 kbar at 630 °C (Li et al., 2017).  
304 This path was interpreted as burial in a subduction zone after tectonic erosion and before continent-  
305 continent collision (Massonne and Li, 2020). However, the Malpica-Tuy zone is a major strike-  
306 slip structure (Díez Fernández and Martínez Catalán, 2012), so that it could be argued that  
307 eventually oblique collision of continental plates played a role. In any case, an uncertainty range  
308 must be considered for the estimation of both the upper pressure (20 kbar) and lower pressure  
309 (suggested as 12 kbar) limits for continental rocks involved in continental subduction.

310 The aforementioned steeply dipping subduction of continental material in case of an oblique  
311 continent-continent collision (Fig. 5) rapidly brings this material to great depths and, thus, results  
312 in burial paths that are characterized by a clear pressure increase at only slightly rising temperature  
313 (Fig. 3). On the contrary, the beginning of (shallow) subduction of continental material on top of

314 the oceanic crust or in the tip of the downgoing continental plate leads to both rising pressure and  
315 temperature, resulting in P-T paths approximately following geotherms (see figure 2B).

316 Melting of the most deeply subducted continental crust can occur at the highest pressures  
317 reached or during the early uplift of corresponding HP rocks (stage III of figure 5) formed in the  
318 environment of an oblique continent-continent collision. This is implied by Eocene to Miocene  
319 plutons at the Periadriatic Fault System (see Section 2.2) along the Eastern and Central Alps (e.g.,  
320 Ji et al., 2019). The melts of these plutons are of intermediate to acidic calcalkaline character  
321 (dominantly tonalitic-granodioritic) and are, thus, geochemically similar to plutons in magmatic  
322 arcs, which are also generated by melting of mantle and continental crust (e.g., von Blanckenburg,  
323 1992; Pamić and Palinkaš, 2000; Bonin, 2004). The uplift process of the addressed HP rocks can  
324 tectonically move them away from the transpressional fault system (see Dewey et al., 1998) and  
325 re-arrange them in a nappe pile, which is, for example, obvious in the Erzgebirge Crystalline  
326 Complex and its surroundings (e.g., Hallas et al., 2021). However, the alignment of calcalkaline  
327 plutons commonly occurs at the suture (major strike-slip fault) of obliquely collided continental  
328 plates, whereas these other plutons are arranged in a zone (magmatic arc) with a considerable  
329 distance to the collision front at frontal collision.

330 Ultrabasic (serpentinized) rocks can occur in various geotectonic environments of continent-  
331 continent collisions. It was pointed out above that (hydrated) mantle rocks were found in  
332 accretionary wedges as well as in suture zones of obliquely collided continental plates. The type  
333 of mantle rock being involved in the accretionary wedge is always a plagioclase- or spinel-bearing  
334 lherzolite (or harzburgite, dunite), whereas garnet peridotite can: (1) become part of the deep  
335 subduction channel with its upwards-directed mass flow (Fig. 2A), and (2) be included in  
336 continental subduction with buoyancy-driven uplift of predominant felsic rocks (Fig. 5). Thus, the

337 occurrence of mantle rocks, which contain either primary spinel or garnet, in suture zones is not  
338 diagnostic for frontal or oblique continent-continent collisions.

### 339 Application to the Chilenia-Gondwana collision

340 Using the above findings and the three P-T paths in figure 3 for metasediments of the  
341 collisional belt formed by the Chilenia-Gondwana collision, it can be suggested that this collision  
342 was oblique. This statement can be hold despite only one (Guarguaraz Complex: Massonne and  
343 Calderón, 2008) of the three paths shows a nearly isothermal burial part, whereas the other two  
344 start very close to the peak pressure. This is compatible with the general observation that the early  
345 metamorphic evolution is usually erased in rocks. The reason for that is the complete reaction of  
346 early formed metamorphic minerals unless they are preserved as inclusions in minerals of the peak  
347 metamorphism. Among these peak metamorphic minerals, garnet predominates generally. In the  
348 rock studied by Massonne and Calderón (2008), an early garnet formed at relatively low pressures  
349 (8 kbar; see figure 3) and was preserved in further growing garnet of the peak-pressure  
350 metamorphism. In principle, other minerals can also be preserved in garnet and contribute to the  
351 understanding of the early metamorphic evolution. As we broadly have to rely on garnet as  
352 container to preserve early formed minerals, it must be considered that this mineral suffers from  
353 overstepping its stability field during prograde metamorphic evolution (Castro and Spear, 2017;  
354 Spear, 2017). The consequence is that a late formation of garnet in a metamorphic rock can prevent  
355 the important preservation of early formed minerals. Then, one cannot recognize whether the  
356 prograde path towards peak-pressure conditions is characterized by a nearly isothermal pressure  
357 increase or a P-T evolution approximately along an isotherm as the cyan and dark orange paths in  
358 figure 2B.

359

360 Before finally judging if a continent-continent collision was frontal or oblique, other criteria  
361 should be considered. In case of the Devonian Chilenia-Gondwana collision, it can be noted that  
362 ultrabasic bodies are related to the HP metasediments (Boedo et al., 2021, and references therein).  
363 However, a metasediment-serpentinite relation is not diagnostic for frontal or oblique continent-  
364 continent collisions as pointed out in the previous section.

365 The geotectonic position of plutons composed predominantly of calcalkaline tonalite to  
366 granodiorite is another point as also outlined in the previous section. The Devonian calcalkaline  
367 plutons in the Frontal Cordillera (Section 3.2) might follow the Chilenia-Gondwana suture,  
368 although they were considered as magmatic arc by Dahlquist et al. (2022). In context with the  
369 unknown extension of Chilenia south of 39° S, the interpretation of the Devonian plutons of  
370 Chaitenia (Hervé et al., 2018) should be also reconsidered. In fact, they were also interpreted as  
371 part of a magmatic arc, but they could instead mark the suture of an oblique collision with  
372 involvement of, for example, a southern part of Chilenia. This would, however, require a  
373 displacement of the alignment of the Devonian plutons in the 39–41° S latitude range (see the  
374 speculative strike-slip fault in figure 4). Metamorphic rocks in the San Carlos de Bariloche area  
375 point to a collisional event in the Devonian (Martínez et al., 2012). The question is whether the  
376 medium-grade HP metasediments (Martínez et al., 2012; Oriolo et al., 2019) there can be, indeed,  
377 related to a collision of Chilenia and Gondwana. Oriolo et al. (2019) determined monazite ages at  
378 about 300 Ma for these rocks, which seem to exclude that these HP rocks formed by the Chilenia  
379 collision. However, monazite ages rather indicate the youngest orogenic events (e.g., Li et al.,  
380 2025). Thus, the aforementioned multiple collisional events in the accretion of microplates in the  
381 southern part of South America could have obscured a Devonian age for the addressed HP rocks.

382

383 The reason for the oblique collision of Chilenia with Gondwana could be the northward  
384 movement (relative to the present geographical orientation) of North America (Laurentia) with  
385 respect to South America (Gondwana) in the Palaeozoic. The corresponding plates were probably  
386 never separated by a wide ocean in this period but rather by small oceanic basins. An oblique  
387 continent-continent collision occurred when such a basin was closed. Afterwards, a new basin  
388 opened leaving a microcontinent (including Pampia and Cuyania: e.g., Martin et al., 2020) attached  
389 to Gondwana behind during the northward movement of Laurentia. Such a scenario would be  
390 consistent with previous ideas by Dalla Salda et al. (1992), Dalziel (1997), and others suggesting  
391 that the collisions of Pampia and Cuyania with Gondwana in the early Palaeozoic were oblique as  
392 well. An indication could be that these collisions did not lead to HP rocks with peak pressures of  
393 more than 20 kbar (e.g., Willner et al., 2023) and eclogite bodies as typical for frontal continent-  
394 continent collisions (see Section 2.1), but a detailed scrutiny of the literature in regard to the  
395 metamorphic evolution of rocks at the boundaries of Pampia and Cuyania and their geotectonic  
396 setting is outside the scope of this study. Laurentia moved so far northwards in the Carboniferous  
397 that a frontal oceanic-continental collision became possible leading to the formation of the Chilean  
398 accretionary wedges.

## 399 **Conclusions**

400 The following conclusions result from this study: 1) Oblique continent-continent collisions  
401 in the Phanerozoic are more common than usually thought. 2) This type of collision can be  
402 recognized by a P-T path that shows an early metamorphic evolution characterized by nearly  
403 isothermal burial and peak pressures in the range of approximately 12 to 20 kbar. 3) The  
404 occurrence of ultrabasic (serpentinized) rocks in the range of suture zones of obliquely collided  
405 continental plates are common. Excellent examples are the ophiolite-rich orogens related to the

406 India-Eurasia collision, such as the Indo-Burman ranges. However, ultrabasic rocks can be also  
407 involved in an accretionary wedge or the type of extrusion wedge, which contains deeply  
408 subducted crustal material and hydrated mantle as a result of frontal collision. 4) The formation of  
409 a chain of calcalkaline plutonic bodies is not typical of frontal or oblique continent-continent  
410 collisions. However, the positions of such chains are different because the one at the suture zone  
411 points to oblique collisions, whereas those 100-300 km (magmatic arc) from this suture (trench  
412 during oceanic and continental plate collision) characterize frontal collisions. Moreover, the chain  
413 of calcalkaline plutons forms just after continental subduction, whereas the magmatic arc develops  
414 already before a frontal continent-continent collision. 5) The collision of Chilenia with SW  
415 Gondwana was probably oblique. 6) There is a certain probability that Chilenia extends to 40.5°  
416 S. A further extension to the south after a speculative displacement to the west in the late Devonian  
417 - early Carboniferous cannot be ruled out.

#### 419 **Acknowledgments**

420 The first author thanks particularly Francisco (Pancho) Hervé, to whom this study is  
421 dedicated, for the chance to explore a fossil accretionary wedge system and magmatic arc by  
422 several field excursions in Chile and also for his open mind in regard to strange geotectonic ideas.  
423 The revision of an earlier version of the manuscript benefited from review reports of four  
424 anonymous colleagues and the editorial handling by Mauricio Calderón, who kindly translated the  
425 abstract into Spanish.

#### 427 **References**

428 Agard, P.; Handy, M.R. 2021. Ocean subduction dynamics in the Alps. *Elements* 17: 9-16.  
429 <https://doi.org/10.2138/gselements.17.1.9>

- 430 Bianchi, F.D.; Martínez, J.C.; Massonne, H.-J.; Delpino, S.H.; Dristas, J.A. 2024. Metamorphic P-  
431 T-d evolution path of ductile-sheared rocks of Cerro Catedral, North Patagonian Andes  
432 of Argentina: From high-P/T Late Paleozoic progression to low-P/T Jurassic overprint.  
433 Journal of South American Earth Sciences 149: 105216.  
434 <https://doi.org/10.1016/j.jsames.2024.105216>
- 435 Boedo, F.L.; Willner, A.P.; Vujovich, G. I.; Massonne, H.-J. 2016. High pressure/low temperature  
436 metamorphism in the collision zone between the Chilenia and Cuyania microcontinents  
437 (Western Precordillera, Argentina). Journal of South American Earth Sciences 72: 227-  
438 240.
- 439 Boedo, F.L.; Pérez Luján, S.; Ariza, J.P.; Vujovich, G.I. 2021. The mafic-ultramafic belt of the  
440 Argentine Precordillera: A geological synthesis. Journal of South American Earth  
441 Sciences 110: 103354. <https://doi.org/10.1016/j.jsames.2021.103354>
- 442 Bonin, B. 2004. Do coeval mafic and felsic magmas in post-collisional to within-plate regimes  
443 necessarily imply two contrasting, mantle and crustal, sources? A review. Lithos 78: 1-  
444 24. <https://doi.org/10.1016/j.lithos.2004.04.042>
- 445 Bonnet, G.; Chopin, C.; Locatelli, M.; Kylander-Clark, A.; Hacker, B.R. 2022. Protracted  
446 subduction of the European hyperextended margin revealed by rutile U-Pb  
447 geochronology across the Dora-Maira massif (western Alps). Tectonics 41:  
448 e2021TC007170. <https://doi.org/10.1029/2021TC007170>
- 449 Bosse, V.; Godard, G.; Devidal, J. L.; Mallens, J.; Shea, T. 2024. Two metamorphic cycles  
450 recorded by monazite in eclogite-facies gneisses (Southern Armorican Massif, France):  
451 A Cambro-Ordovician continental crust involved in eo-Variscan subduction. BSGF Earth  
452 Sciences Bulletin 195: 20, 18 pages. <https://doi.org/10.1051/bsgf/2024018>
- 453 Casquet, C.; Dahlquist, J.A.; Verdecchia, S.O.; Baldo, E.G.; Galindo, C.; Rapela, C.W.; Pankhurst,  
454 R.J.; Morales, M.M.; Murra, J.A.; Fanning, C.M. 2018. Review of the Cambrian Pampean  
455 orogeny of Argentina; a displaced orogen formerly attached to the Saldania Belt of South  
456 Africa? Earth-Science Reviews 177: 209-225.
- 457 Casquet, C.; Ramacciotti, C.; Larrovere, M.A.; Verdecchia, S.; Murra, J.; Baldo, E.G.; Pankhurst,  
458 R.J.; Rapela, C.W. 2021. The Rinconada phase: A regional tectono-metamorphic event  
459 of Silurian age in the pre-Andean basement of Argentina. Journal of South American  
460 Earth Sciences 111: 103432. <https://doi.org/10.1016/j.jsames.2021.103432>

461

462

463 Castro, A.E.; Spear, F.S. 2017. Reaction overstepping and re-evaluation of peak P–T conditions  
464 of the blueschist unit Sifnos, Greece: implications for the Cyclades subduction zone.  
465 *International Geology Review* 59: 548-562.

466 Dahlquist, J.A.; Morales Cámara, M.M.; Alasino, P.H.; Tickyj, H.; Basei, M.A.S.; Galindo, C.;  
467 Moreno, J.A.; Rocher, S. 2022. Geochronology and geochemistry of Devonian  
468 magmatism in the Frontal Cordillera (Argentina): geodynamic implications for the pre-  
469 Andean SW Gondwana margin. *International Geology Review* 64: 233-253.

470 Dahlquist, J.A.; Ramacciotti, C.D., Morales Cámara, M.M.; Basei, M.A.S.; Santos da Cruz, G.;  
471 Gonzalez, G.A. 2025. The 40th anniversary of the Chilenia terrane: where is its Grenville-  
472 age basement? *Journal of South American Earth Sciences* 164: 105638,

473 Dalla Salda, L.H.; Dalziel, I.W.D.; Cingolani, C.A.; Varela, R. 1992. Did the Taconic  
474 Appalachians continue into southern South America? *Geology* 20: 1059-1062.

475 Dal Piaz, G.V.; Bistacchi, A.; Massironi, M. 2003. Geological outline of the Alps. *Episodes* 26:  
476 175-180.

477 Dalziel, I.W.D. 1997. Neoproterozoic-Paleozoic geography and tectonics: review, hypothesis,  
478 environmental speculation. *Geological Society of America Bulletin* 109: 16-42.

479 Davis, J.; Roeske, S.; McClelland, W.; Snee, L. 1999. Closing the ocean between the Precordillera  
480 terrane and Chilenia: Early Devonian ophiolite emplacement and deformation in the  
481 southwest Precordillera. *In* *Laurentia and Gondwana Connections before Pangea* (Ramos,  
482 V.; Keppie, J.; editors). *Geological Society of America Special Papers* 336: 115-138.

483 Dallanave, E. 2024. Assessing the reliability of paleomagnetic datasets using the R package  
484 PmagDiR. *Scientific Reports* 14: 1666. <https://doi.org/10.1038/s41598-024-52001-x>

485 Deckart, K.; Hervé, F.; Fanning, C.N.; Ramírez, V.; Calderón, M.; Godoy, E. 2014. U-Pb  
486 geochronology and Hf-O isotopes of zircons from the Pennsylvanian Coastal Batholith,  
487 South-Central Chile. *Andean Geology* 41: 49-82.

488 De Hoog, J.C.M.; Janák, M; Vrabec, M.; Froitzheim, N. 2009. Serpentinised peridotites from an  
489 ultrahigh-pressure terrane in the Pohorje Mts. (Eastern Alps, Slovenia): Geochemical  
490 constraints on petrogenesis and tectonic setting. *Lithos* 109: 209-222.  
491 <https://doi.org/10.1016/j.lithos.2008.05.006>

492

493

494

495 Dewey, J. F.; Holdsworth, R.E.; Strachan, R.A. 1998. Transpression and Transtension Zones. *In*  
496 Continental Transpressional and Transtensional Tectonics (Holdsworth, R.E.; Strachan,  
497 R.A.; Dewey, J.E.; editors). Geological Society of London Special Publications 135: 1-  
498 14. <https://doi.org/10.1144/GSL.SP.1998.135.01.01>

499 Dhital, M.R. 2015. Introduction. *In* Geology of the Nepal Himalaya. (Dhital, M.R.; editor), 1-10.  
500 Regional Geology Reviews, Springer, Cham. [https://doi.org/10.1007/978-3-319-02496-](https://doi.org/10.1007/978-3-319-02496-7_1)  
501 [7\\_1](https://doi.org/10.1007/978-3-319-02496-7_1)

502 Díez Fernández, J.; Martínez Catalán, J.R. 2012. Stretching lineations in high-pressure belts: the  
503 fingerprint of subduction and subsequent events (Malpica-Tui complex, NW Iberia).  
504 Journal of the Geological Society 169: 531-543.

505 Ernst, W.G. 2005. Alpine and Pacific styles of Phanerozoic mountain building: subduction-zone  
506 petrogenesis of continental crust. Terra Nova 17: 165-188.

507 Franke, W. 2000. The mid-European segment of the Variscides: tectonostratigraphic units, terrane  
508 boundaries and plate tectonic evolution. *In* Orogenic processes: Quantification and  
509 Modelling in the Variscan Belt (Franke, W.; Haak, V.; Oncken, O.; Tanner, D.; editors).  
510 Geological Society of London Special Publications 179: 35-61.

511 Gilotti, J.A. 2013. The realm of ultrahigh-pressure metamorphism. Elements 9: 255-260.

512 Godard, G. 2001. The Les Essarts eclogite-bearing metamorphic Complex (Vendée, southern  
513 Armorican Massif, France): Pre-Variscan terrains in the Hercynian belt? Geologie de la  
514 France 1-2: 19-51.

515 Gregori, D.A.; Bjerg, E.A. 1997. New evidence on the nature of the Frontal Cordillera ophiolitic  
516 belt-Argentina. Journal of South American Earth Sciences 10: 147-155.

517 Gregori, D.A.; Kostadinoff, J.; Strazzere, L.; Raniolo, A. 2008. Tectonic significance and  
518 consequences of the Gondwanide orogeny in northern Patagonia, Argentina. Gondwana  
519 Research 14: 429-450.

520 Gregori, D.A.; Kostadinoff, J.; Alvarez, G.; Raniolo, A.; Strazzere, L.; Martínez, J. C., Barros, M.  
521 2013. Preandean geological configuration of the eastern North Patagonian Massif,  
522 Argentina. Geoscience Frontiers 4 : 693-708. doi: 10.1016/j.gsf.2013.01.001

523 Groppo, C.; Ferrando, S.; Gilio, M.; Botta, S.; Nosenzo, F.; Balestro, G., Festa, A.; Rolfo, F. 2019.  
524 What's in the sandwich? New P–T constraints for the (U)HP nappe stack of southern  
525 Dora-Maira Massif (Western Alps). European Journal of Mineralogy 31: 665-683.

526

527 Hallas, P.; Pfänder, J.A.; Kroner, U.; Sperner, B. 2021. Microtectonic control of  $^{40}\text{Ar}/^{39}\text{Ar}$  white  
528 mica age distributions in metamorphic rocks (Erzgebirge, N-Bohemian Massif)  
529 Constraints from combined step heating and multiple single grain total fusion  
530 experiments. *Geochimica et Cosmochimica Acta* 314: 178-208.

531 Handy, M.R.; Babist, J.; Wagner, R.; Rosenberg, C.; Konrad, M. 2005. Decoupling and its relation  
532 to strain partitioning in continental lithosphere: insight from the Periadriatic fault system  
533 (European Alps). *Geological Society of London Special Publications* 243: 249-276.  
534 <https://doi.org/10.1144/GSL.SP.2005.243.01.17>

535 Handy, M.R.; Schmid, S.M.; Bousquet, R.; Kissling, E.; Bernoulli, D. 2010. Reconciling plate-  
536 tectonic reconstructions of Alpine Tethys with the geological–geophysical record of  
537 spreading and subduction in the Alps. *Earth Science Reviews* 102: 121-158.

538 Harlow, G.E.; Tsujimori, T.; Sorensen, S.S. 2015. Jadeitites and plate tectonics. *Annual Review*  
539 *of Earth and Planetary Sciences* 43: 105-138. [https://doi.org/10.1146/annurev-earth-](https://doi.org/10.1146/annurev-earth-060614-105215)  
540 [060614-105215](https://doi.org/10.1146/annurev-earth-060614-105215)

541 Heredia, N.; Folguera, A. 2025. Introduction to the scientific ideas of Professor Victor A. Ramos  
542 on the Proterozoic and Paleozoic geotectonic evolution of the Argentinean-Chilean  
543 Andes: origin, evolution, and alternatives. *Journal of South American Earth Sciences*,  
544 166: 105713. <https://doi.org/10.1016/j.jsames.2025.105713>

545 Hervé, F. 1988. Late Paleozoic subduction and accretion in Southern Chile. *Episodes* 11: 183-188.

546 Hervé, F.; Calderón, M.; Fanning, C.M.; Pankhurst, R.J.; Godoy, E. 2013. Provenance variations  
547 in the Late Paleozoic accretionary complex of central Chile as indicated by detrital  
548 zircons. *Gondwana Research* 23: 1122-1135. <https://doi.org/10.1016/j.gr.2012.06.016>

549 Hervé, F.; Calderón, M.; Fanning, C.M.; Pankhurst, R.J.; Fuentes, F.; Rapela, C.W.; Correa, J.;  
550 Quezada, P.; Marambio, C. 2016. Devonian magmatism in the accretionary complex of  
551 southern Chile. *Journal of the Geological Society* 173: 587-602.  
552 <https://doi.org/10.1144/jgs2015-163>

553 Hervé, F.; Calderón, M.; Fanning, M.; Pankhurst, R.; Rapela, C.W.; Quezada, P. 2018. The country  
554 rocks of Devonian magmatism in the North Patagonian Massif and Chaitenia. *Andean*  
555 *Geology* 45: 301. <https://doi.org/10.5027/andgeoV45n3-3117>

556

557

558

- 559 Hyppolito, T.; García-Casco, A.; Juliani, C.; Meira, V.T.; Hall, C. 2014. Late Paleozoic onset of  
560 subduction and exhumation at the western margin of Gondwana (Chilena Terrane):  
561 Counterclockwise P–T paths and timing of metamorphism of deep-seated garnet-mica  
562 schist and amphibolite of Punta Sirena, Coastal Accretionary Complex, central Chile (34°  
563 S). *Lithos* 206-207: 409-434.
- 564 Iaccarino, S.; Montomoli, C.; Carosi, R.; Massonne, H.-J.; Langone, A.; Visonà, D. 2015.  
565 Pressure–temperature–time–deformation path of kyanite-bearing migmatitic paragneiss  
566 in the Kali Gandaki valley (Central Nepal): Investigation of Late Eocene–Early Oligocene  
567 melting processes. *Lithos* 231: 103-121.
- 568 Ji, W.-Q.; Malusà, M.G.; Tiepolo, M.; Langone, A.; Zhao, L.; Wu, F.-Y. 2019. Synchronous  
569 Periadriatic magmatism in the Western and Central Alps in the absence of slab breakoff.  
570 *Terra Nova* 31: 120-128. <https://doi.org/10.1111/ter.12377>
- 571 Kaneko, Y.; Katayama, I.; Yamamoto, H.; Misawa, K.; Ishikawa, M.; Rehman, H.U.; Kausar,  
572 A.B.; Shiraishi, K. 2003. Timing of Himalayan ultrahigh-pressure metamorphism:  
573 sinking rate and subduction angle of the Indian continental crust beneath Asia. *Journal of*  
574 *Metamorphic Geology* 21: 589-599.
- 575 Kröner, A.; Willner, A.P. 1998. Time of formation and peak of Variscan HP-HT metamorphism  
576 of quartz-feldspar rocks in the central Erzgebirge, Saxony, Germany. *Contributions to*  
577 *Mineralogy and Petrology* 132: 1-20.
- 578 Kroner, U.; Roscher, M.; Romer, R.L. 2016. Ancient plate kinematics derived from the  
579 deformation pattern of continental crust: Paleo- and Neo-Tethys opening coeval with  
580 prolonged Gondwana–Laurussia convergence. *Tectonophysics* 681: 220-233.
- 581 Kryl, J.; Jeřábek, P.; Lexa, O. 2021. From subduction channel to orogenic wedge: Exhumation  
582 recorded by orthogneiss microstructures in Erzgebirge, Bohemian Massif.  
583 *Tectonophysics* 820: 229096.
- 584 Li, B.; Massonne, H.-J.; Opitz, J. 2017. Clockwise and anticlockwise P-T paths of high-pressure  
585 rocks from the 'La Pioza' eclogite body of the Malpica-Tuy zone, NW Spain. *Journal of*  
586 *Petrology* 58: 1363-1392.
- 587 Li, B.; Massonne, H.-J.; Koller, F.; Zhang, J. 2021. Metapelite from the high- to ultrahigh-pressure  
588 terrane of the Eastern Alps (Pohorje Mountains, Slovenia) - New pressure, temperature  
589 and time constraints on a polymetamorphic rock. *Journal of Metamorphic Geology* 39:  
590 695-726.

591

- 592 Li, B.; Massonne, H.-J.; Yuan, X. 2023. Wealth of P-T-t information from metasediments in the  
593 HP-UHP terrane of the Pohorje Mountains, Slovenia, elucidates the evolution of the  
594 Eastern Alps. *Journal of Metamorphic Geology* 41: 1167-1196.
- 595 Li, B.; Massonne, H.-J.; Zhang, J.; Yuan, X.; Luo, T. 2025. Monazite beats zircon regarding dating  
596 of young metamorphic events – an example from polycyclic granitic gneiss of the Pohorje  
597 Mountains, Slovenian Alps. *Terra Nova* 37: 111-118.
- 598 Liu, Y.; Siebel, W.; Massonne, H.-J.; Xiao, X. 2007. Geochronological and petrological  
599 constraints for tectonic evolution of the Central Greater Himalayan Sequence in the  
600 Kharta area, Southern Tibet. *The Journal of Geology* 115: 215-230.
- 601 López, V.; Gregori, D.A. 2004. Provenance and evolution of the Guarguaraz Complex, Cordillera  
602 Frontal, Argentina. *Gondwana Research* 7: 1197-1208.
- 603 López de Azarevich, V.L.; Escayola, M.; Azarevich, M.B.; Pimentel, M.M.; Tassinari, C. 2009.  
604 The Guarguaraz Complex and the Neoproterozoic-Cambrian evolution of southwestern  
605 Gondwana: geochemical signatures and geochronological constraints. *Journal of South  
606 American Earth Sciences* 28: 333-344.
- 607 MaksaeV, V.; Munizaga, F.; Tassinari, C. 2014. Timing of the magmatism of the paleo-Pacific  
608 border of Gondwana: U–Pb geochronology of Late Paleozoic to Early Mesozoic igneous  
609 rocks of the north Chilean Andes between 20° and 31°S. *Andean Geology* 41: 447-506.
- 610 Marcos, P.; Renda, E.M.; González, P.D.; Oriolo, S.; Scivetti, N.; Benedini, L.; GeraIdes, M.;  
611 Gregori, D.; Yoya, M.B.; Bahía, M. 2023. Devonian to Early Carboniferous retreating—  
612 Advancing subduction switch in the northwestern Patagonia Accretionary Orogen: U-Pb  
613 and Lu-Hf isotopic insights. *Tectonics* 42: e2022TC007533.  
614 <https://doi.org/10.1029/2022TC007533>
- 615 Martin, E.L.; Collins, W. J.; Spencer, C.J. 2020. Laurentian origin of the Cuyania suspect terrane,  
616 western Argentina, confirmed by Hf isotopes in zircon. *Geological Society of America  
617 Bulletin* 132: 273-290. <https://doi.org/10.1130/B35150.1>
- 618 Martínez, J.C.; Dristas, J.A.; Massonne, H.-J. 2012. Paleozoic accretion of the microcontinent  
619 Chilena, North Patagonian Andes: High-pressure metamorphism and subsequent thermal  
620 relaxation. *International Geology Review* 54: 472-490.
- 621 Massonne, H.-J. 2011. Pre-conference field trip: Erzgebirge (Ore Mountains), Germany and Czech  
622 Republic; German part of the Saxonian Erzgebirge. *Geolines* 23: 29-59.
- 623

624 Massonne, H.-J. 2013. Constructing the pressure-temperature path of ultrahigh-pressure rocks.  
625 Elements 9: 267-272.

626 Massonne, H.-J. 2015. Derivation of P-T paths from high-pressure metagranites - examples from  
627 the Gran Paradiso Massif, western Alps. Lithos 226: 265-279.

628 Massonne, H.-J. 2023. A new type of saidenbachite with pseudomorphs after coesite phenocrysts  
629 from the north-western Bohemian Massif, Germany. Terra Nova 35: 379-387.

630 Massonne, H.-J. 2024a. Eclogite with biotite porphyroblasts – which conditions are responsible  
631 for their formation? An example from the northern Fleur-de-Lys Supergroup,  
632 Newfoundland, Canada. Journal of Metamorphic Geology 42: 291-318.

633 Massonne, H.-J. 2024b. Pressure-temperature-time evolution of a polymetamorphic paragneiss  
634 with pseudomorphs after jadeite from the HP-UHP Gneiss-Eclogite Unit of the Variscan  
635 Erzgebirge Crystalline Complex, Germany. Journal of Metamorphic Geology 42: 1159-  
636 1178.

637 Massonne, H.-J.; Calderón, M. 2008. P-T evolution of metapelites from the Guarguaraz Complex,  
638 Argentina: evidence for Devonian crustal thickening close to the western Gondwana  
639 margin. Revista Geológica de Chile 35: 215-231.

640 Massonne, H.-J.; Li, B. 2020. Zoning of eclogitic garnet cores – a key pattern demonstrating the  
641 dominance of tectonic erosion as part of the burial process of worldwide occurring  
642 eclogites. Earth-Science Reviews 210: 103356.  
643 <https://doi.org/10.1016/j.earscirev.2020.103356>

644 Massonne, H.-J.; Li, B. 2022. Eclogite with unusual atoll garnet from the southern Armorican  
645 Massif, France: pressure-temperature path and geodynamic implications. Tectonophysics  
646 823: 229183.

647 Massonne, H.-J.; O'Brien, P.J. 2003. The Bohemian Massif and the NW Himalaya. In Ultrahigh  
648 Pressure Metamorphism (Carswell, D.A.; Compagnoni, R.; editors). European  
649 Mineralogical Union, Notes in Mineralogy 5: 145-187.

650 Massonne, H.-J.; Willner, A.P. 2008. Phase relations and dehydration behaviour of psammopelite  
651 and mid-ocean ridge basalt at very-low-grade to low-grade metamorphic conditions.  
652 European Journal of Mineralogy 20: 867-879.

653

654

655

656 Mpodozis, C.; Ramos, V.A. 1990. The Andes of Chile and Argentina. *In* *Geology of the Andes*  
657 *and its Relation to Hydrocarbon and Mineral Resources* (Ericksen, G.E.; Cañas Pinochet,  
658 M.T.; Reinemund, J.A.; editors). Circum-Pacific Council for Energy and Mineral  
659 Resources, Earth Science Series 11: 59-90.

660 Müller, R.D.; Cannon, J.; Qin, X.; Watson, R.J.; Gurnis, M.; Williams, S.; Pfaffelmoser, T.; Seton,  
661 M.; Zahirovic, S. 2018. GPlates: Building a virtual Earth through deep time.  
662 *Geochemistry, Geophysics, Geosystems* 19: 2243-2261.  
663 <https://doi.org/10.1029/2018GC007584>

664 Muñoz-Montecinos, J.; Cambeses, A.; Angiboust, S. 2024. Accretion and subduction mass transfer  
665 processes: Zircon SHRIMP and geochemical insights from the Carboniferous Western  
666 Series, Central Chile. *International Geology Review* 66: 54-80.

667 Naing, T.T.; Robinson, S.A.; Searle, M.P.; Morley, C.K.; Millar, I.; Green, O.R.; Bown, P.R.;  
668 Danelian, T.; Petrizzo, M.R.; Henderson, G.M. 2023. Age, depositional history and  
669 tectonics of the Indo-Myanmar Ranges, Myanmar. *Journal of the Geological Society* 180.  
670 <https://doi.org/10.1144/jgs2022-091>

671 Nyunt, T.T.; Massonne, H.-J.; Sun, T.T. 2017. Jade and adjacent high-pressure metamorphic rocks  
672 from the Jade Mines Belt, Tawmaw area, Kachin State, northern Myanmar. *In* *Myanmar:*  
673 *Geology, Resources and Tectonics* (Barber, A.J.; Zaw, K.; Crow, M.J.; editors).  
674 Geological Society of London Memoirs 48: 297-317.

675 O'Brien, P.J.; Zotov, N.; Law, R.; Khan, M.A.; Jan, M.Q. 2001. Coesite in Himalayan eclogite and  
676 implications for models of India-Asia collision. *Geology* 29: 435-438.

677 Oriolo, S.; Schulz, B.; González, P.D.; Bechis, F.; Olaizola, E.; Krause, J.; Renda, E.; Vizán, H.  
678 2019. The Late Paleozoic tectonometamorphic evolution of Patagonia revisited: Insights  
679 from the pressure-temperature-deformation-time (P-T-D-t) path of the Gondwanide  
680 basement of the North Patagonian Cordillera (Argentina). *Tectonics* 38: 2378-2400.

681 Ovung, T.N.; Ghosh, B.; Ray, J. 2021. Petrogenesis of neo-Tethyan ophiolites from the Indo-  
682 Myanmar ranges: a review. *International Geology Review* 63: 1437-1449.  
683 <https://doi.org/10.1080/00206814.2020.1775137>

684 Paffrath, M.; Friederich, W.; Schmid, S.M.; Handy, M.R.; the AlpArray and AlpArray-Swath D  
685 Working Group 2021. Imaging structure and geometry of slabs in the greater Alpine area  
686 – a P-wave travel-time tomography using AlpArray Seismic Network data. *Solid Earth*  
687 12: 2671-2702.

688

689 Palin, R.M.; Reuber, G.S.; White, R.W.; Kaus, B.J.; Weller, O.M. 2017. Subduction  
690 metamorphism in the Himalayan ultrahigh-pressure Tso Moriri massif: an integrated  
691 geodynamic and petrological modelling approach. *Earth and Planetary Science Letters*  
692 467: 108-119.

693 Pamić, J.; Palinkaš, L. 2000. Petrology and geochemistry of Paleogene tonalites from the  
694 easternmost parts of the Periadriatic Zone. *Mineralogy and Petrology* 70: 121-141.

695 Pankhurst, R.; Rapela, C.; Fanning, C.; Márquez, M. 2006. Gondwanide continental collision and  
696 the origin of Patagonia. *Earth-Science Reviews* 76: 235-257.

697 Plissart, G.; González-Jiménez, J.M.; Garrido, L.N.F.; Colás, V.; Berger, J.; Monnier, C.; Diot, H.;  
698 Padrón-Navarta, J. A. 2019. Tectono-metamorphic evolution of subduction channel  
699 serpentinites from South-Central Chile. *Lithos* 336-337: 221-241.

700 Plissart, G., Moral Jilorm, J. C., González-Jiménez, J. M., Muñoz-Montecinos, J., Pavez Salgada,  
701 C., Rivera Herrera, A.; Cabrera Bermúdez, F.; Marchesi, C.; Corgne, A.; Moreno-Abril,  
702 A.J.; Lanari, P.; Berger, J.; Halton, A. 2026. Birth, life and death of the Devonian  
703 Chaitenia back-arc along the Southwestern Gondwanan margin (southern Chile).  
704 *Gondwana Research* 149: 17-43.

705 Ramos, V.A. 1988. Late Proterozoic-Early Paleozoic of South America: A collisional history.  
706 *Episodes* 11: 168-174.

707 Ramos, V.A.; Naipauer, M. 2014. Patagonia. Where does it come from? *Journal of Iberian*  
708 *Geology* 40: 367-379.

709 Rangin, C.; Maurin, T.; Masson, F. 2013. Combined effects of Eurasia/Sunda oblique convergence  
710 and East-Tibetan crustal flow on the active tectonics of Burma. *Journal of Asian Earth*  
711 *Sciences* 76: 185-194. <https://doi.org/10.1016/j.jseaes.2013.05.018>

712 Rapalini, A.E. 2005. The accretionary history of southern South America from the latest  
713 Proterozoic to the Late Palaeozoic: some palaeomagnetic constraints. *In* *Terrane*  
714 *Processes at the Margins of Gondwana* (Vaughan, A.P.; Leat, P.T.; Pankhurst, R.J.;  
715 editors). Geological Society of London, Special Publications, 246, 305-328.

716 Rapalini, A.E.; López de Luchi, M.; Martínez Dopico, C.; Lince Klinger, F.; Giménez, M.;  
717 Martínez, P. 2010. Did Patagonia collide with Gondwana in the Late Paleozoic? Some  
718 insights from a multidisciplinary study of magmatic units of the North Patagonian Massif.  
719 *Geologica Acta* 8: 349-371.

720

- 721 Rapela, C.W.; Hervé, F.; Pankhurst, R.J.; Calderón, M.; Fanning, C.M.; Quezada, P., Poblete, F.;  
722 Palape, C.; Reyes, T. 2021. The Devonian accretionary orogen of the North Patagonian  
723 cordillera. *Gondwana Research* 96: 1-21. <https://doi.org/10.1016/j.gr.2021.04.004>
- 724 Richter, P.P.; Ring, U.; Willner, A.P.; Leiss, B. 2007. Structural contacts in subduction complexes  
725 and their tectonic significance: The Late Paleozoic coastal accretionary wedge of central  
726 Chile. *Journal of the Geological Society of London* 164: 203-214.
- 727 Serra-Varela, S.; Heredia, N.; Giacosa, R.; García-Sanseguno, J.; Farias, P. 2022. Review of the  
728 polyorogenic Palaeozoic basement of the Argentinean North Patagonian Andes: age,  
729 correlations, tectonostratigraphic interpretation and geodynamic evolution. *International*  
730 *Geology Review* 64: 72-95.
- 731 Slavinski, H.; Morris, B.; Ugalde, H.; Spicer, B.; Skulski, T.; Rogers, N. 2010. Integration of  
732 lithological, geophysical, and remote sensing information: a basis for remote predictive  
733 geological mapping of the Baie Verte Peninsula, Newfoundland. *Canadian Journal of*  
734 *Remote Sensing* 36: 99-118.
- 735 Spear, F.S. 2017. Garnet growth after overstepping. *Chemical Geology* 466: 491-499.
- 736 Stampfli, G.M. 2000. Tethyan oceans. *In* *Tectonics and Magmatism in Turkey and Surrounding*  
737 *Area* (Bozkurt, E.; Winchester, J.A.; Piper, J.D.A.; editors). Geological Society of  
738 London Special Publications 173: 1-23.
- 739 Teyssier, C.; Tikoff, B.; Markley, M. 1995. Oblique plate motion and continental tectonics.  
740 *Geology* 23: 447-450.
- 741 Thomas, W.A.; Astini, R.A. 1996. The Argentine Precordillera: A traveler from the Ouachita  
742 embayment of North American Laurentia. *Science* 273: 752-757.
- 743 Tricart, P.; Schwartz, S. 2006. A north-south section across the Queyras Schistes lustrés (Piedmont  
744 zone, Western Alps): Syn-collision refolding of a subduction wedge. *Eclogae Geologica*  
745 *Helvetica* 99: 429-442. <https://doi.org/10.1007/s00015-006-1197-6>
- 746 van der Voo, R. 1990. The reliability of paleomagnetic data. *Tectonophysics* 184: 1-9.
- 747 van Staal, C.R.; Zagorevski, A. 2020. Accretion, soft and hard collision: Similarities, differences  
748 and an application from the Newfoundland Appalachian Orogen. *Geoscience Canada* 47:  
749 103-118.
- 750 van Staal, C.R.; Whalen, J.B.; Valverde-Vaquero, P.; Zagorevski, A.; Rogers, N. 2009. Pre-  
751 Carboniferous, episodic accretion-related, orogenesis along the Laurentian margin of the  
752 northern Appalachians. *In* *Ancient Orogens and Modern Analogues* (Murphy, J.B.;

753 Keppie, J.D.; Hynes, A.J.; editors). Geological Society of London Special Publication  
754 327: 271-316.

755 Varela, R.; Cingolani, C.A.; Passarelli, C.R.; Basei, M.A.S. 2005. El basamento cristalino de los  
756 Andes Norpatagónicos en Argentina: geocronología e interpretación tectónica. *Revista*  
757 *Geológica de Chile* 32: 167-187. <https://doi.org/10.5027/andgeoV32n2-a01>.

758 von Blanckenburg, F.; Früh-Green, G.; Diethelm, K.; Stille, P. 1992. Nd-, Sr-, O-isotopic and  
759 chemical evidence for a two-stage contamination history of mantle magma in the Central-  
760 Alpine Bergell intrusion. *Contributions to Mineralogy and Petrology* 110; 33-45.

761 Vujovich, G.I.; van Staal, C.R.; Davis, W. 2004. Age constraints on the tectonic evolution and  
762 provenance of the Pie de Palo Complex, Cuyania Composite Terrane, and the Famatinian  
763 orogeny in the Sierra de Pie de Palo, San Juan, Argentina. *Gondwana Research* 7: 1041-  
764 1056.

765 Werner, O.; Lippolt, H.J. 2000. White mica  $^{40}\text{Ar}/^{39}\text{Ar}$  ages of the Erzgebirge metamorphic rocks:  
766 simulating the chronological results by a model of Variscan crustal imbrication. *In*  
767 *Orogenic Processes: Quantification and Modelling in the Variscan Belt* (Franke, W.;  
768 Haak, V.; Oncken, O.; Tanner, D.; editors). Geological Society of London Special  
769 Publications 179: 323-336.

770 Williams, H. 1979. The Appalachian orogen in Canada. *Canadian Journal of Earth Sciences* 16:  
771 792-807.

772 Willner, A.P.; Hervé, F.; Massonne, H.-J. 2000. Mineral chemistry and pressure-temperature  
773 evolution of two contrasting high-pressure-low-temperature belts in the Chonos  
774 Archipelago, Southern Chile. *Journal of Petrology* 41: 309-330.

775 Willner, A.P.; Glodny, J.; Gerya, T.V.; Godoy, E.; Massonne, H.-J. 2004. A counterclockwise PTt  
776 path of high-pressure/low-temperature rocks from the Coastal Cordillera accretionary  
777 complex of south-central Chile: constraints for the earliest stage of subduction mass flow.  
778 *Lithos* 75: 283-310.

779 Willner, A.P.; Thomson, S.N.; Kröner, A.; Wartho, J.; Wijbrans, J.R.; Hervé, F. 2005. Time  
780 Markers for the Evolution and Exhumation History of a Late Palaeozoic Paired  
781 Metamorphic Belt in North–Central Chile (34°–35°30'S). *Journal of Petrology* 46: 1835-  
782 1858. <https://doi.org/10.1093/petrology/egi036>

783

784

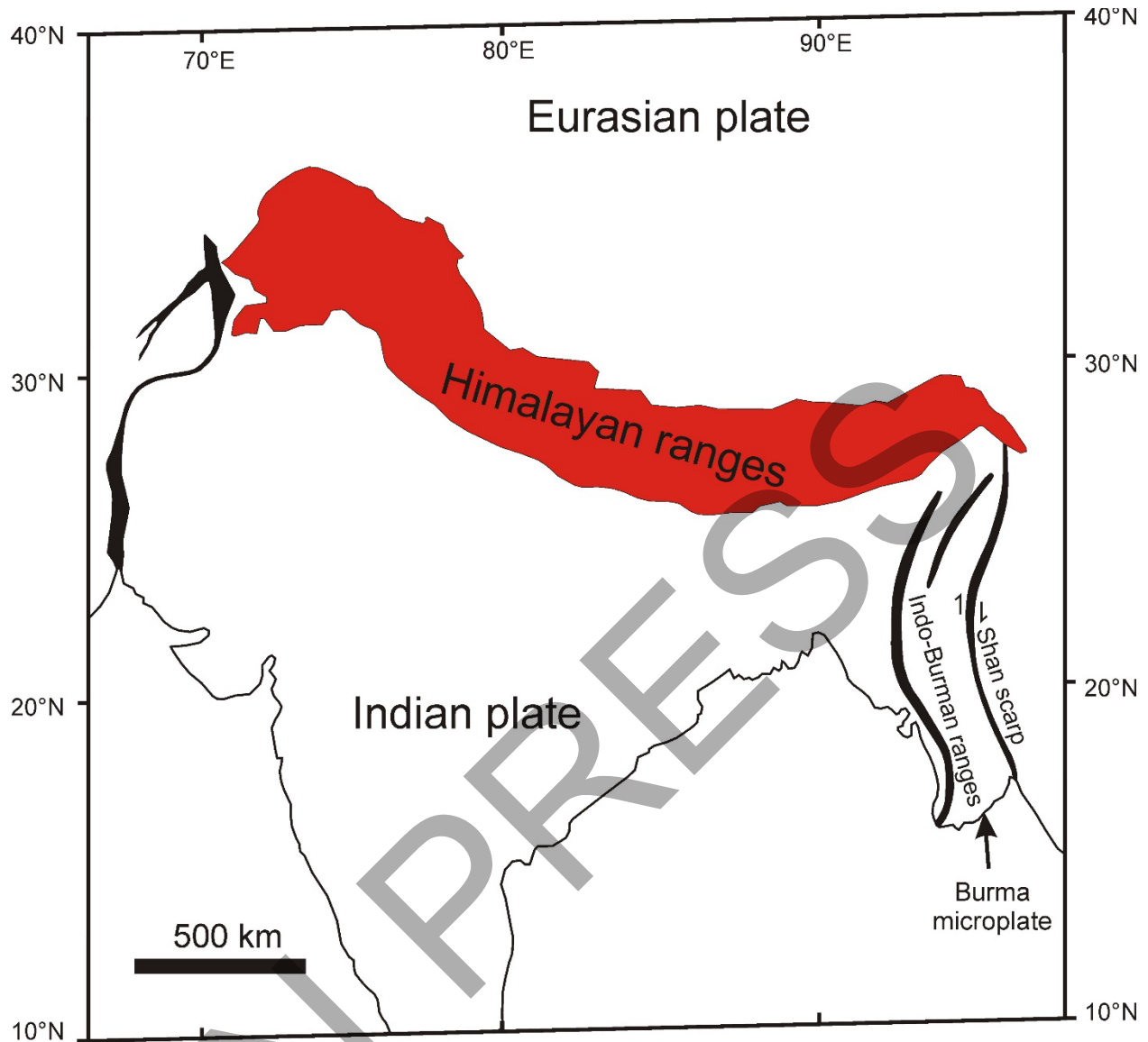
785 Willner, A.P.; Gerdes, A.; Massonne, H.-J.; Schmidt, A.; Sudo, M.; Thomson, S.N.; Vujovich, G.  
786 2011. The geodynamics of collision of a microplate (Chilena) in Devonian times deduced  
787 by the pressure-temperature time evolution within part of a collisional belt (Guarguaraz  
788 Complex, W-Argentina). *Contribution to Mineralogy and Petrology* 162: 303-327.

789 Willner A.P.; Anczkiewicz, R.; Glodny, J.; Pohlner, J. E.; Sudo, M.; van Staal, C.R.; Vujovich,  
790 G.I. 2023. Interrelated pressure-temperature-time-paths of medium to high pressure  
791 metamorphic rocks in the Sierra Pie de Palo (W-Argentina): Evolution of a “hard”  
792 collisional wedge during an Ordovician microcontinent-arc collision. *Tectonophysics*  
793 859: 229861. <https://doi.org/10.1016/j.tecto.2023.229861>

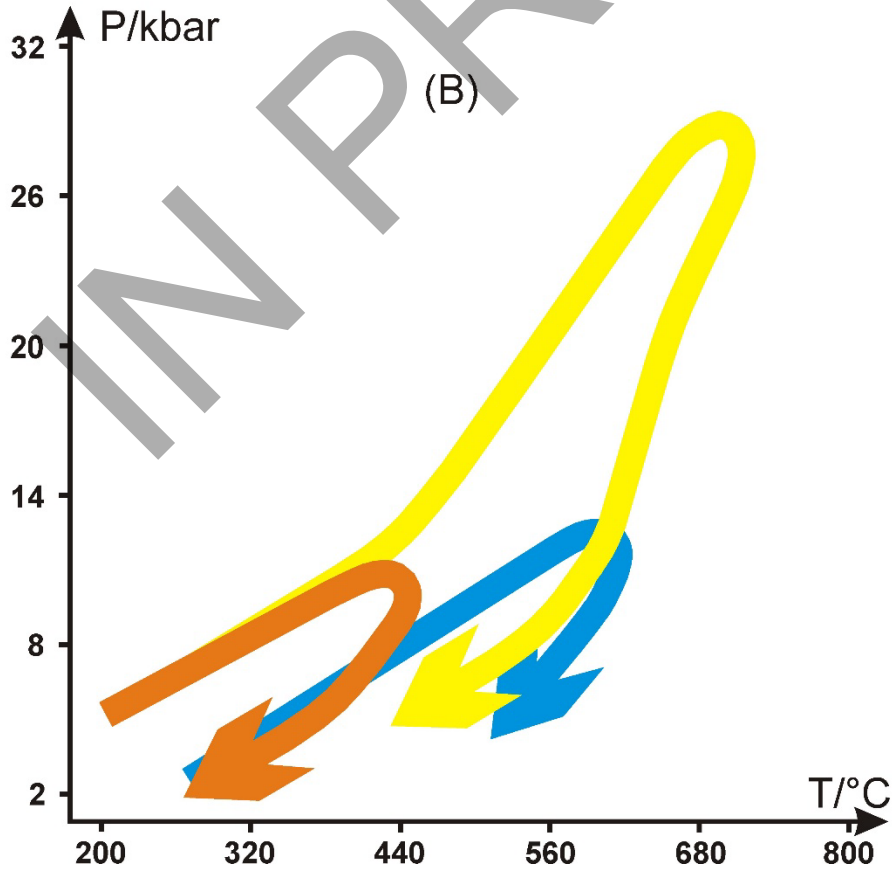
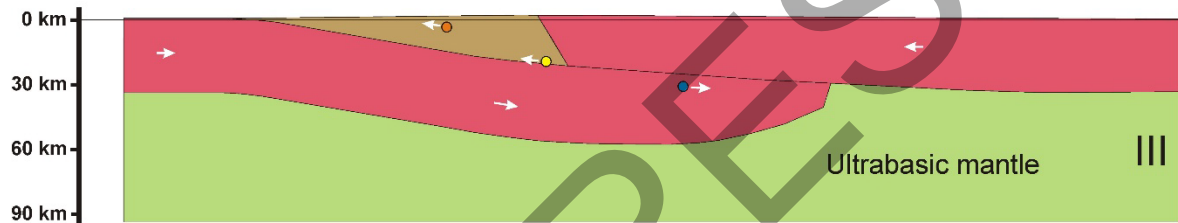
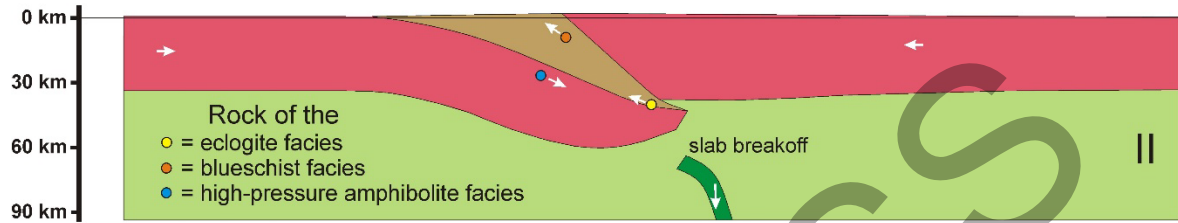
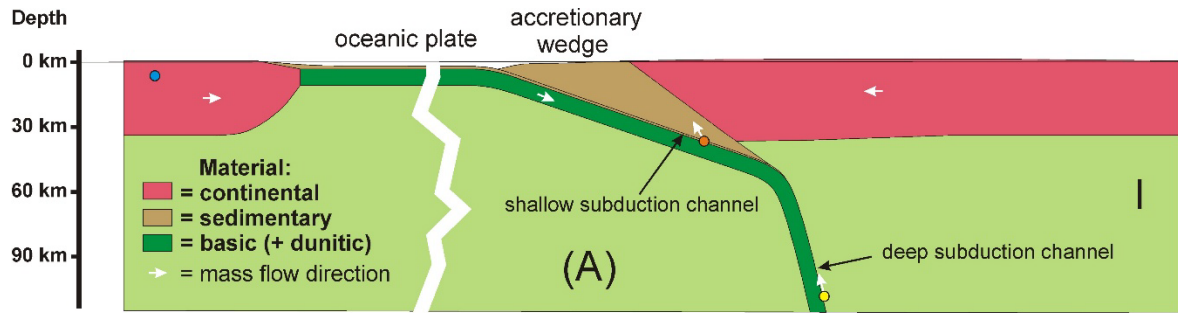
794 Willner, A.P.; Boedo, F.; Vujovich, G.I. 2025. Discussion on: “The 40th anniversary of the  
795 Chilena terrane: Where is its Grenville-age basement?” by J.A. Dahlquist, C. D.  
796 Ramacciotti, M.M. Morales Cámara, M.A.S. Basei, G.Santos da Cruz, G. A. Gonzalez  
797 [Journal of South American Earth Sciences 164 (2025) 105638]. *Journal of South*  
798 *American Earth Sciences* 168: 105844. <https://doi.org/10.1016/j.jsames.2025.105844>

799 Yoya, M.B.; Oriolo, S.; González, P.; Restelli, F.; Renda, E.; Bechis, F.; Newbery, J.C.; Marcos, P.;  
800 Olaizola, E. 2023. The birth of the Gondwanide arc: Insights into Carboniferous  
801 magmatism of the North Patagonian Andes (Argentina). *Journal of South American Earth*  
802 *Sciences* 123: 104225. <https://doi.org/10.1016/j.jsames.2023.104225>

803  
804  
805  
806  
807  
808  
809  
810  
811  
812  
813  
814

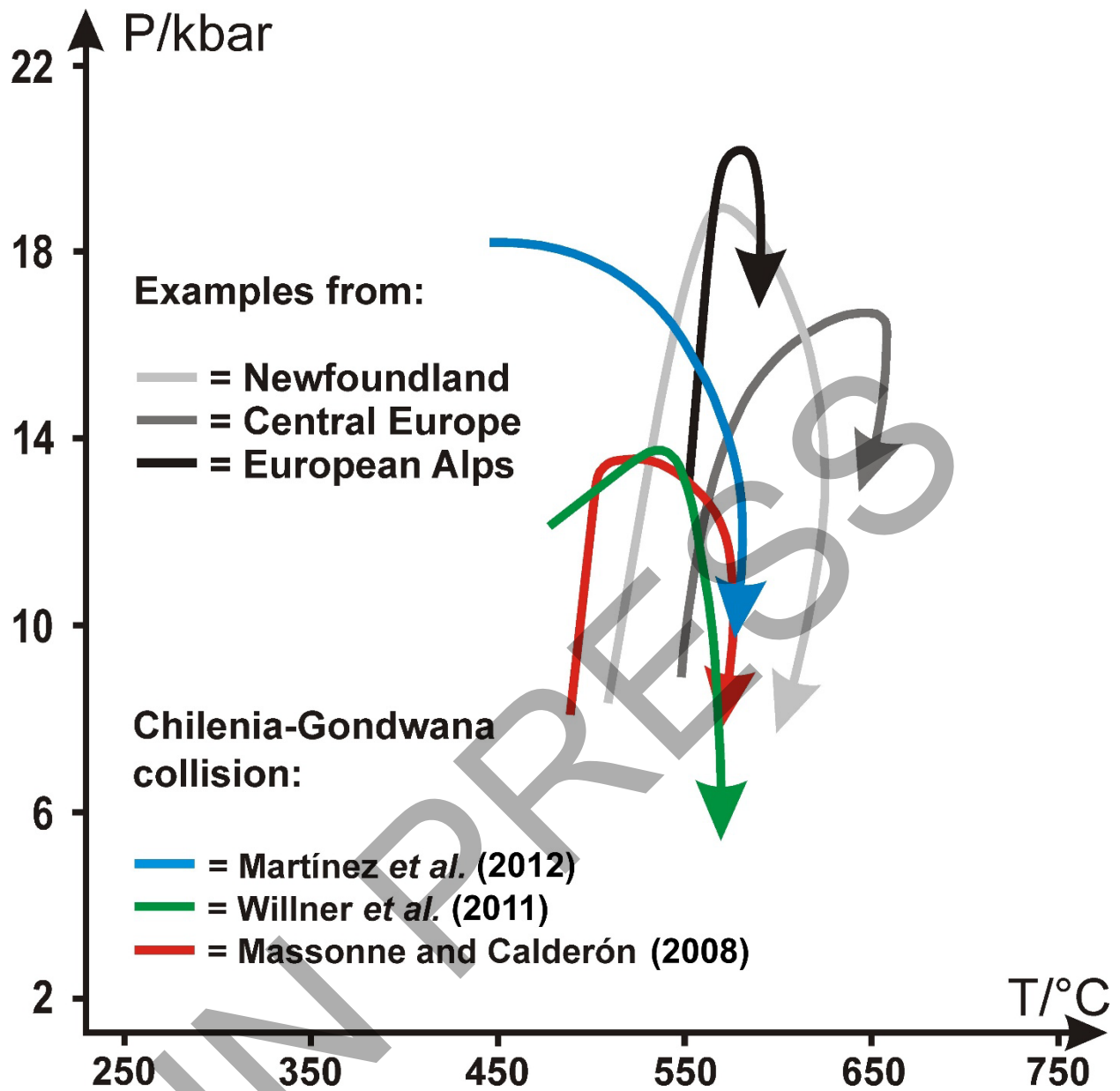


815  
 816 **Fig. 1.** Geotectonic situation after the collision of the Indian and Eurasian plates modified after  
 817 Dhital (2015). The Himalayan ranges resulting from this collision are shown in red. “Ophiolites,  
 818 their klippen, and associated rocks“ (Dhital, 2015) are presented in black. Among the black areas  
 819 is the Shan scarp that is related to the Sagaing Fault, a major strike-slip fault (see the half arrows).



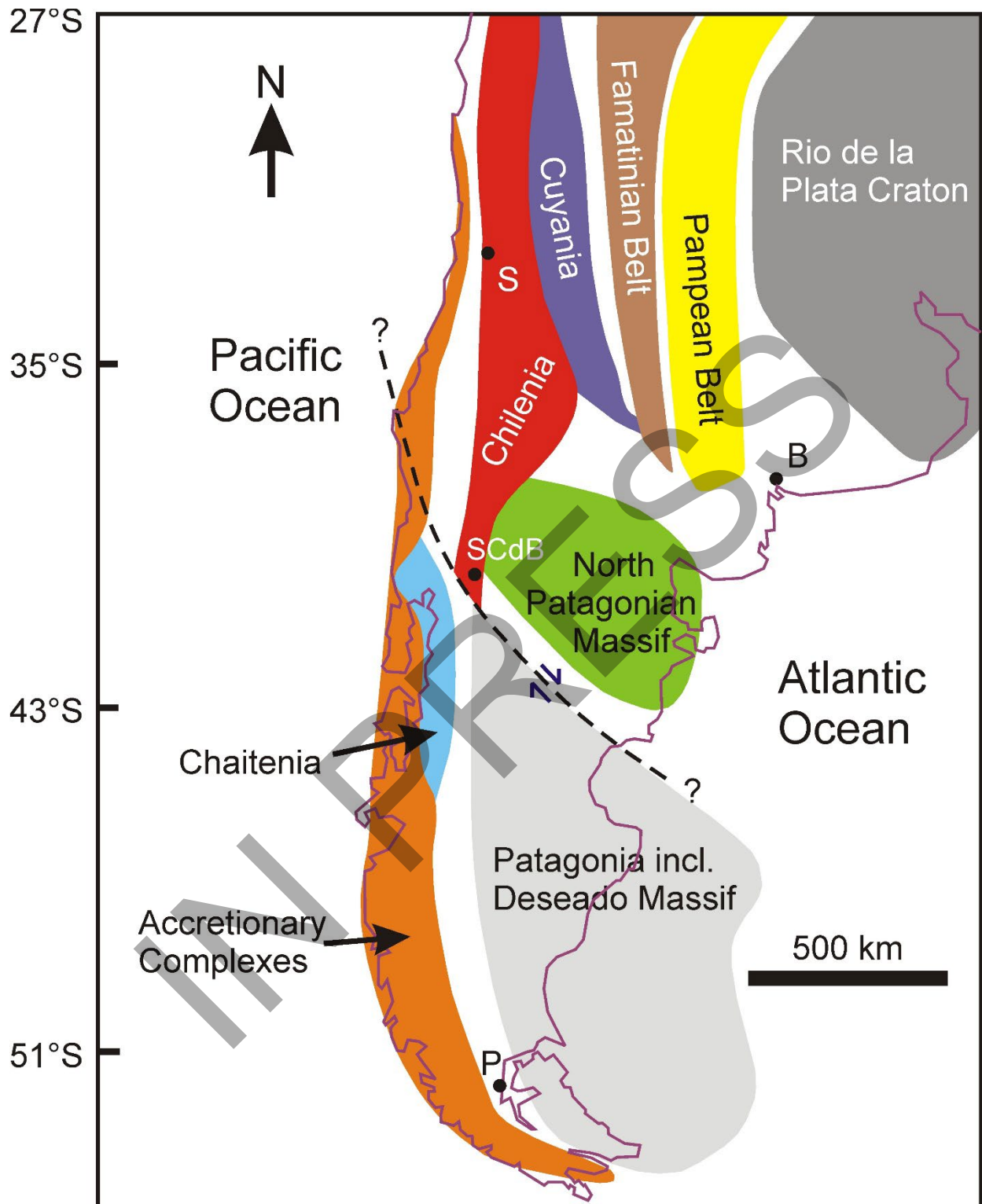
821 **Fig. 2. A.** Geotectonic scenario of a typical frontal collision of continental plates (stages II and III)  
822 that was preceded by subduction of an oceanic plate (stage I) between these continental plates. **B.**  
823 Typical P-T paths for the three rock markers in A. The colours of these paths are the same as the  
824 related markers. The rock (yellow) that is deeply subducted and exhumed in the deep subduction  
825 channel reached very high peak pressures (29 kbar is already in the realm of ultrahigh-pressure  
826 metamorphism). The rock (dark orange) that was involved in the accretionary wedge by basal  
827 accretion (see the Chilean example in Section 3.2) was metamorphosed at blueschist-facies  
828 conditions. The rock (cyan) in the downgoing plate during continent-continent collision, reached  
829 similar peak pressures (around 11 kbar), however, at clearly higher temperatures and, thus, at the  
830 high-pressure amphibolite facies.

IN PRESS



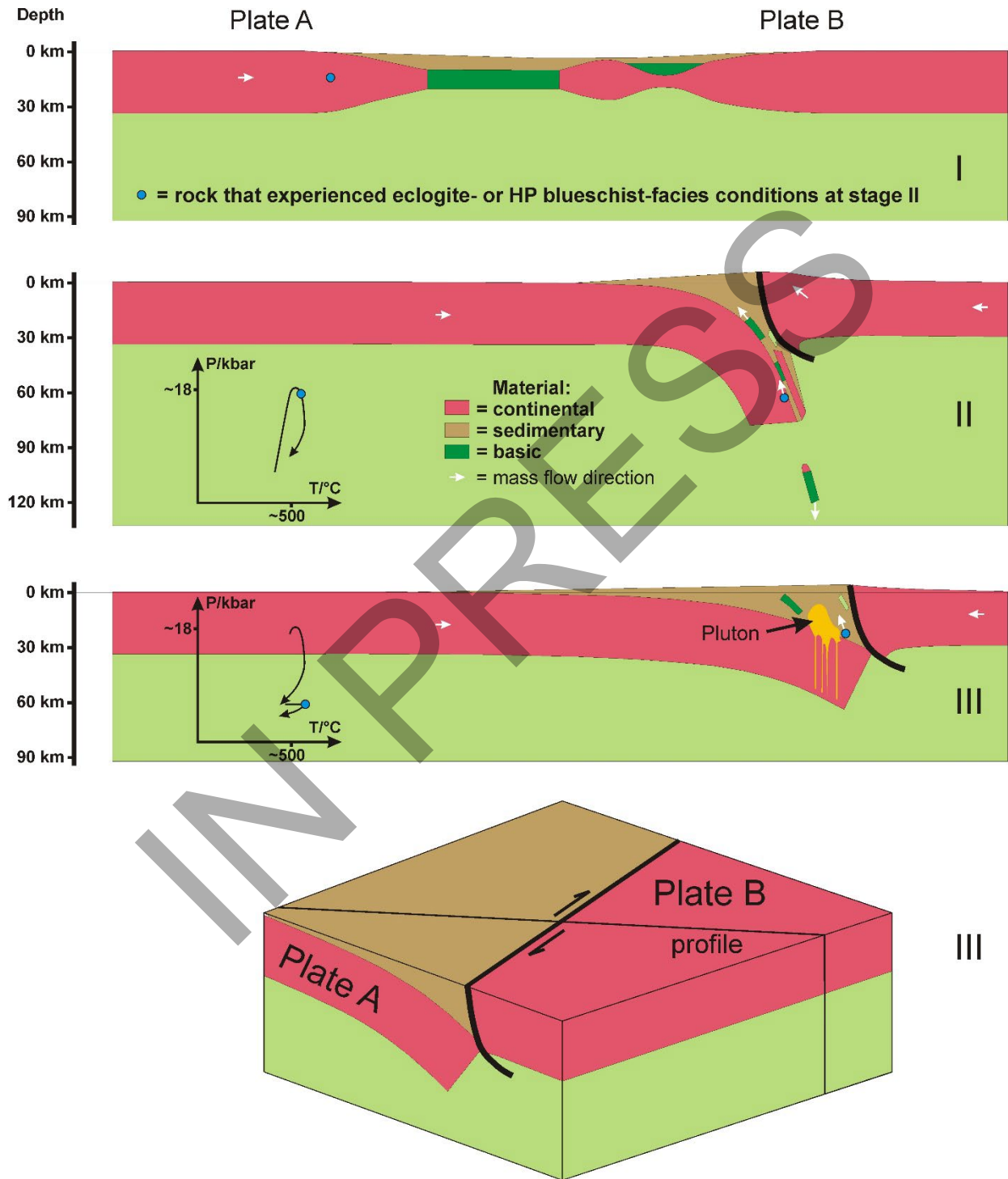
831  
 832 **Fig. 3.** P-T paths that were derived for various high-pressure (HP) metamorphic rocks (for sources  
 833 see text). In colour: studied rocks resulting from the collision of Chilenia with SW Gondwana (see  
 834 Section 3.2). In different grey tones: two paths for Palaeozoic HP metamorphic rocks (see Section  
 835 2.3) and one for Cenozoic ones (European Alps, Section 2.2) being examples for oblique continent-  
 836 continent collisions.

837



838  
 839 **Fig. 4.** Geotectonic structure of the southern part of South America mainly in terms of accreted  
 840 microplates (modified after Hervé et al., 2018). Differing from the original, the area of Chilienia  
 841 could have been extended to the south as argued in the text. The strike-slip fault (broken line) is

842 purely speculative concerning position and movement in the Late Devonian-early Carboniferous.  
 843 Black dots mark towns (B: Bahía Blanca, P: Punta Arenas, SCdB: San Carlos de Bariloche) and  
 844 the city of Santiago de Chile (S).



845  
 846 **Fig. 5.** Geotectonic scenario of an oblique continent-continent collision modified after Li et al.  
 847 (2023). A small oceanic basin or proto-oceanic crust develops in an extensional tectonic regime to

848 its maximum width at stage I. Afterwards, this basin is closed by obliquely approaching continental  
849 plates A and B. This process culminates in the generation of a major transpressional strike-slip  
850 fault system (thick black line in the profiles and block diagram) and steep subduction of Plate A  
851 (called here continental subduction). The other plate is rather obducting simultaneously.  
852 Continental subduction (stage II) is followed by the ascent of continental material but further  
853 subduction of basic (+mantle) eclogitized material. A relevant P-T path for the subducted  
854 continental material (cyan marker) is shown on the left-hand side. The rock presented by the cyan  
855 marker experiences contact metamorphism (stage III, which refers to the block diagram as well)  
856 at relatively low pressures as it is located close to a pluton (see P-T path). This pluton is fed by  
857 intermediate to acidic melts generated at deep levels of the subducted continental crust probably  
858 also influenced by mantle fluids.

IN PRESS